Dissolution Equilibria and Kinetics of Fluorite and Calcite Mixtures

Minerals commonly contain impurities, and their dissolution involves complicated ionic equilibria and multicomponent mass transfer. This paper describes the experiments that were carried out and proposes a mechanism for dissolution behavior of fluorspar containing calcite as a major impurity in both batchwise and continuous packed-bed systems.

The mechanism is based on analysis of coupled equilibria among the soluble species. Of more than eight potentially relevant species, only three (*viz.*, F^-, HCO_3^-, and Ca^{2+}) are significant. The coupled flux equations for F^- and HCO_3^- are written in terms of "main" and "cross" mass transfer coefficients, with the concentration of Ca^{2+} being accounted for by electroneutrality. Only one main mass transfer coefficient needs to be determined experimentally; and other coefficients can be evaluated from it by means of simple diffusion coefficient ratios, which are determined independently. The Stanton number based on the main mass transfer coefficient is correlated with Reynolds number and the Schmidt number for packed bed dissolution.

Jian Qi
Kent S. Knaebel
Department of Chemical Engineering
Ohio State University
Columbus, OH 43210

Introduction

Multicomponent mass transfer at a fluid and solid interface can be found in many chemical engineering processes such as leaching, dissolution or crystallization, electrolysis, and adsorption, as well as chemical reactions involving solid reactants or porous catalysts. Consequently, it has long been a focus of studies in many different disciplines (Wendt, 1965; Woolf, 1972; Stewart and Prober, 1964; Stewart, 1973; Cussler, 1976; Anderson and Graf, 1976; Taylor, 1982; Smith and Taylor, 1983; Pinto and Graham, 1987). But most of the previous work centered either on the sole aspect of multicomponent diffusion or on the mathematical treatments of convective processes under well-defined conditions. Relatively little work has been published on multicomponent mass transfer operations involving convection and complicated boundary conditions, much less for situations that are normally encountered, such as in batch and fixed bed operations.

Since Toor (1964) introduced multicomponent mass transfer coefficients, little effort has been devoted to their applications. This is because prevalent process conditions involve concentration gradients that are difficult to measure or predict; hence, the coefficients are not easily accessible from measured flux. Nevertheless, extensive correlations have already been established for single mass transfer coefficients. Incentives for developing multicomponent mass transfer correlations exist when cross-term mass transfer cannot be neglected, i.e., when the flux of one component may be affected by the concentration gradient of another. This is especially true in electrolyte solutions, where the interactions among ionic species lead to a relatively large cross-term effects.

Dissolution of calcium fluoride or fluorspar (i.e., fluorite with various impurities) has been the subject of many studies because of the roles that the former has played in dental care, and due to the prevalence of latter and its impact on geology and mineralogy (Maier and Bellack, 1957; Maier, 1960; Brown and Roberson, 1977; Diniz et al., 1982; Bruun et al., 1983; Lagerlof et al., 1988; others are reviewed by Qi, 1988). The primary inducement for this study has evolved from a combination of the previous reasons: fluorspar may be an alternate, inherently safe and inexpensive water fluoridation source. Actually, if a mineral source of pure CaF_2 were readily available, no such study would be necessary because there are few subtleties involved in dissolution of a pure solid. Conversely, since common sources of fluorspar contain calcite as a major impurity (Bates, 1969), its dissolution produces more than two aqueous species and must be treated as a multicomponent mass transfer system (Qi, 1988).

The purpose of the present study is to combine the complex

Correspondence concerning this paper should be addressed to K. S. Knaebel.

equilibria and multicomponent diffusion concepts that are inherent to mineral dissolution to develop a mathematical model that is applicable to a wide variety of conditions and geometries.

Equilibrium Analysis

Dissolution equilibrium of fluorspar containing calcite is similar to that of a CaF_2-$CaCO_3$ mixture, where the major heterogeneous dissolution reactions are:

$$CaF_2(s) \rightleftharpoons Ca^{2+} + 2F^- \quad K_{sp1} \tag{1}$$

$$CaCO_3(s)(\text{calcite}) \rightleftharpoons Ca^{2+} + CO_3^{2-} \quad K_{sp2} \tag{2}$$

Also occurring are the following reactions in the aqueous phase that affect the above two:

$$CO_2(aq) + H_2O \rightleftharpoons H^+ + HCO_3^- \quad K_{a1} \tag{3}$$

$$HCO_3^- \rightleftharpoons H^+ + CO_3^{2-} \quad K_{a2} \tag{4}$$

$$CaF^+ \rightleftharpoons Ca^{2+} + F^- \quad K_b \tag{5}$$

$$CaHCO_3^+ \rightleftharpoons Ca^{2+} + HCO_3^- \quad K_c \tag{6}$$

$$H_2O \rightleftharpoons H^+ + OH^- \quad K_w \tag{7}$$

where Eq. 3 is a combination of the two reactions below:

$$CO_2(aq) + H_2O \rightleftharpoons H_2CO_3 \tag{3a}$$

$$H_2CO_3 \rightleftharpoons H^+ + HCO_3^- \tag{3b}$$

In these equations, the constant that follows each reaction is the equilibrium constant for that reaction, defined as the product of product activities divided by product of reactant activities. Note that the activities of both the solid and water are taken as unity.

Besides the above reactions, there are actually some other reactions occurring in the liquid phase to form species such as HF, HF_2^-, $Ca(HCO_3)_2$, $CaCO_3^0$, and $CaOH^-$. But effect of these species on the equilibria can be easily shown to be negligible (Qi, 1988). The electroneutrality of the equilibrium solution gives:

$$2[Ca^{2+}] + [CaHCO_3^+] + [CaF^+] + [H^+] = [F^-] + [HCO_3^-] + 2[CO_3^{2-}] + [OH^-] \tag{8}$$

where the brackets [] represent the molar concentration. By employing the equilibrium constants in Eqs. 1 to 7, the equilibrium calcium concentration of this multicomponent system can be expressed as:

$$\begin{aligned} 2[Ca^{2+}] &+ \frac{1}{K_c\gamma_{CaHCO_3^-}}\sqrt{\frac{K_{sp2}K_{a1}[Ca^{2+}]\gamma_{Ca^{2+}}a_{CO_2(aq)}}{K_{a2}}} \\ &+ \frac{1}{K_b\gamma_{CaF^+}}\sqrt{K_{sp1}[Ca^{2+}]\gamma_{Ca^{2+}}} \\ &+ \frac{1}{\gamma_{H^+}}\sqrt{\frac{K_{a1}K_{a2}a_{CO_2(aq)}[Ca^{2+}]\gamma_{Ca^{2+}}}{K_{sp2}}} \\ &= \frac{1}{\gamma_{F^-}}\sqrt{\frac{K_{sp1}}{[Ca^{2+}]\gamma_{Ca^{2+}}}} + \frac{2K_{sp2}}{[Ca^{2+}]\gamma_{Ca^{2+}}\gamma_{CO_3^{2-}}} \\ &+ \frac{1}{\gamma_{HCO_3^-}}\sqrt{\frac{K_{sp2}K_{a1}a_{CO_2(aq)}}{K_{a2}[Ca^{2+}]\gamma_{Ca^{2+}}}} \\ &+ \frac{K_w}{\gamma_{OH^-}}\sqrt{\frac{K_{sp2}}{K_{a1}K_{a2}a_{CO_2(aq)}[Ca^{2+}]\gamma_{Ca^{2+}}}} \end{aligned} \tag{9}$$

where γ_i is the activity coefficient of species i; and $a_{CO_2(aq)}$ is the activity of aqueous carbon dioxide.

The activity coefficients of the ionic species were estimated by the Debye-Hückel theory (Stumm and Morgan, 1981) and the solubility products and equilibrium constants were obtained from literature sources, $pK_{sp1} = 10.3$, $pK_{sp2} = 8.3$ (Snaeyink and Jenkens, 1980); $pK_{a1} = 6.3$, $pK_{a2} = 10.4$ (Larson and Buswell, 1942); $pK_b = 1$ (Butler, 1964); $pK_c = 1$ (Jacobson and Langmuir, 1974). Finally, the activity of aqueous carbon dioxide can be calculated in accordance with the system conditions. If such a system is open to atmosphere, then the activity of aqueous carbon dioxide can be estimated from Henry's law since the atmospheric carbon dioxide partial pressure is known to be 0.00033 ± 0.00001 atm (Weast et al., 1986). This results in $a_{CO_2(aq)} = 0.013$ mM (Stumm and Morgan, 1981). Thus, Eq. 9 can be solved for $[Ca^{2+}]$, and the results have been shown by Qi (1988) to agree closely with experimental measurements for open systems at various temperatures and initial pH and calcium ion backgrounds.

An order of magnitude analysis for an open system indicates that only species F^-, HCO_3^-, and Ca^{2+} are necessary in analysis. Thus, Eq. 9 is virtually equivalent to:

$$[Ca^{2+}] = \left(\frac{1}{2\gamma_{F^-}}\sqrt{\frac{K_{sp1}}{\gamma_{Ca^{2+}}}} + \frac{1}{2\gamma_{F^-}}\sqrt{\frac{K_{sp2}K_{a1}(a_{CO_2(aq)})}{K_{a2}\gamma_{Ca^{2+}}}}\right)^{2/3} \tag{10}$$

A comparison of the exact solution (Eq. 9) with the approximate solution (Eq. 10) is shown in Figure 1 for a range of aqueous carbon dioxide activities. Since the discrepancies are negligible except at very low concentration of aqueous carbon dioxide, the

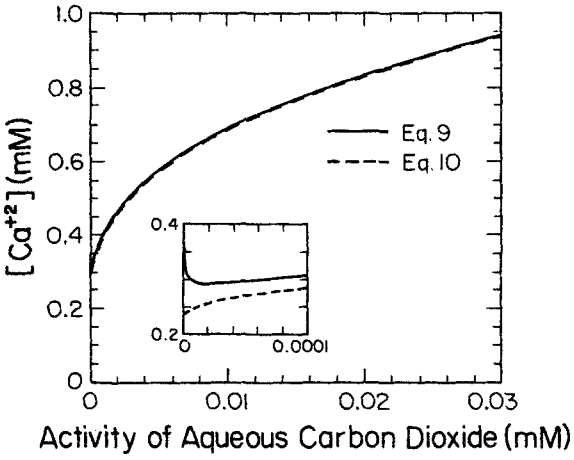

Figure 1. Equilibrium calcium concentration calculated *from Eqs. 9 and 10 as a function of saturation* activity of aqueous carbon dioxide.

open system of fluorspar dissolution equilibrium (*viz.*, $a_{CO_2(aq)} = 0.0013$ mM) can be treated as a dilute ternary system consisting of F^-, HCO_3^-, and Ca^{2+}.

Coupled Flux Equations and Their Solutions

An inherent feature of a batch system open to the atmosphere is that it is in continual equilibrium with ambient CO_2. Similarly, when considering a packed column, if the influent water is equilibrated with the atmosphere and its residence time in the column is short, it can also be treated approximately as an open system, i.e., with CO_2 at equilibrium between atmosphere and water.

Because open-system dissolution of fluorspar can be treated as a ternary system of F^-, HCO_3^-, and Ca^{2+}, in terms of equilibrium calculatioin, as Eq. 10 shows, a similar relationship is expected for their molar fluxes, since the concentration gradient between the solid surface and the bulk solution largely determines the relative magnitude of each ionic flux. If species F^-, HCO_3^-, and Ca^{2+} are designated by 1, 2, and 3, respectively, electroneutrality of the system requires:

$$2J_3 = J_1 + J_2 \tag{11}$$

where J_i is the molar flux of species i with respect to the molar average velocity. By neglecting conveyance effects, these are identical to the fluxes with respect to fixed coordinates, i.e., the solid surface.

The fluxes of F^- and HCO_3^- are considered as the two independent fluxes in this study. The multicomponent mass transfer coefficients defined by Toor (1964) can be extended to give:

$$J_1 = k_{11}(C_{1S} - C_1) + k_{12}(C_{2S} - C_2) \tag{12}$$

$$J_2 = k_{21}(C_{1S} - C_1) + k_{22}(C_{2S} - C_2) \tag{13}$$

where C_{is} and C_i are the concentrations of species i on the surface of solid and in the bulk solution, respectively; k_{11} and k_{22} are main mass transfer coefficients, and k_{12} and k_{21} are cross mass transfer coefficients.

For a column packed with soluble solids, a mass balance at steady state can be made on a differential column volume, dV, to yield

$$J_i a(1 - \epsilon)dV = QdC_i \tag{14}$$

where ϵ is the voidage; a is the surface area per unit volume of solid; and Q is the interstitial volumetric flow rate.

Substituting Eqs. 12 and 13 into Eq. 14 gives:

$$\frac{Q}{a(1-\epsilon)}\frac{dC_1}{dV} = k_{11}(C_{1S} - C_1) + k_{12}(C_{2S} - C_2) \tag{15}$$

$$\frac{Q}{a(1-\epsilon)}\frac{dC_2}{dV} = k_{21}(C_{1S} - C_1) + k_{22}(C_{2S} - C_2) \tag{16}$$

Let

$$\tau = \alpha(1 - \epsilon)V/Q \tag{17}$$

Since fluorspar is only sparingly soluble, the packing can be assumed uniform. Therefore the voidage is constant. Equations 15 and 16 then become:

$$\frac{dC_1}{d\tau} = k_{11}(C_{1S} - C_1) + k_{12}(C_{2S} - C_2) \tag{18}$$

$$\frac{dC_2}{d\tau} = k_{21}(C_{1S} - C_1) + k_{22}(C_{2S} - C_2) \tag{19}$$

with boundary condition:

$$C_i = C_{i0} \quad \text{at} \quad \tau = 0, (i = 1, 2) \tag{20}$$

where C_{io} represent concentratons at the upstream end of the section considered.

Let

$$\bar{C}_i = \frac{C_i - C_{i0}}{C_{iS} - C_{i0}}, (i = 1, 2) \tag{21}$$

$$C_r = \frac{C_{1S} - C_{10}}{C_{2S} - C_{20}} \tag{22}$$

Assuming constant k_{ij} and then solving Eqs. 18 and 19 by the Laplace transform gives:

$$\bar{C}_1(\tau) = 1 - \exp(B_1\tau) + B_3[\exp(B_2\tau) - \exp(B_1\tau)] \tag{23}$$

$$\bar{C}_2(\tau) = 1 - \exp(B_1\tau) + B_4[\exp(B_2\tau) - \exp(B_1\tau)] \tag{24}$$

where

$$B_1 = -\frac{k_{11} + k_{22}}{2}\left[1 + \sqrt{1 - \frac{4(k_{11}k_{22} - k_{12}k_{21})}{(k_{11} + k_{22})^2}}\right] \tag{25}$$

$$B_2 = -\frac{k_{11} + k_{22}}{2}\left[1 - \sqrt{1 - \frac{4(k_{11}k_{22} - k_{12}k_{21})}{(k_{11} + k_{22})^2}}\right] \tag{26}$$

$$B_3 = \frac{k_{11} + k_{12}/C_r + B_1}{B_2 - B_1} \tag{27}$$

$$B_4 = \frac{k_{21}C_r + k_{22} + B_1}{B_2 - B_1} \tag{28}$$

Essentially identical equations can also be derived for dissolution in a batch system by equating $V_L dC_i$ to $aV_s J_i dt$, as shown by Qi (1988) except the different definitions of the variables used. In a batch system, C_{i0} and C_i, respectively, represent the initial concentration and the instantaneous bulk concentration of species i, and $\tau = a(V_s/V_L)t$, where a is the surface area per unit volume of solid, V_s and V_L are the volumes of dissolving solid and solvent, respectively, and t is the dissolution time.

Experimental Studies

The material used in this study was white or translucent native fluorspar ore from the Rosiclare district of Illinois. Information on this mineral has been given elsewhere (Weller et al., 1952). After gravel and other debris were removed, the fluorspar was crushed and segregated into different size ranges with standard U.S. sieves. The segregated particles appeared in vari-

ous shapes, with aspect ratios roughly from 1 to 4. Prior to their use for experiments, the fluorspar particles were gently washed with distilled water to remove fine powder and dust, and then dried in ambient air. The washed particles were examined with a microscope and found to be virtually dust free.

The chemical composition of the fluorspar was initially analyzed using a wide-angle X-Ray crystallograph to show presence of calcium fluoride, quartz and calcite. The mineral was then further analyzed to indicate that it contained about 97 wt. % CaF_2, 2 wt. % calcite and 1 wt. % quartz.

Batchwise experiments were conducted in a tank stirred with a rotating basket impeller. Suzuki and Kawazoe (1975) performed detailed study of this type of contactor for mass transfer from surface of solid particles to bulk liquid. The basket impeller in this study was constructed of fine-mesh metal screen with three external mixing vanes that induced flow through the basket as it rotated. The basket had a diameter of 5.5 cm and volume of 130 cm^3. It held 70 grams of fluorspar and was immersed in 1,500 mL of distilled water, while rotating at a constant revolution speed. The tank, 14 cm in diameter and 3,000 mL in volume, had three evenly-spaced, 2-cm-wide baffles. During each experiment, samples of 10 mL were pipetted periodically to measure fluoride concentration as a function of time. Experimental data were collected at 210 rpm. (Several preliminary runs indicated that dissolution rate increased when revolution speed increased from 150 to 240 rpm.) After each run, the solid was unloaded from the basket and air dried for reuse. Due to the low solubility of fluorspar, the mass loss and size change of the particles were insignificant. Additional details of the experiments, along with the fluoride concentration-vs.-time data, are given in Table 1.

Table 1. Fluoride Concentration vs. Time in Batch Dissolution Using Rotating Basket Impeller for a Single Sample of Fluorspar Particles*

Time min	Identical Conditions, $[F^-]$, mM						
	Run 1	Run 2	Run 3	Run 4	Run 6	Run 7	Run 11
0	0.0	0.0	0.0	0.0	0.0	0.0	0.0
1	0.023	0.0068	0.0063	0.0049	0.0031	0.0032	—
2	0.041	0.011	0.0095	0.010	0.0059	0.0063	0.0068
3	0.061	0.019	0.014	0.012	0.0095	0.010	0.0095
5	0.088	0.029	0.020	0.017	0.015	0.014	0.015
10	0.113	0.048	0.034	0.029	0.025	0.022	0.023
15	0.143	0.061	0.044	0.037	0.034	—	0.029
20	0.163	0.075	0.051	0.045	0.045	0.036	0.036
30	0.178	0.091	0.064	0.053	0.051	0.052	0.048
35	—	—	—	0.057	—	—	—
45	0.190	0.113	0.075	0.072	0.066	0.061	0.061
75	—	—	—	0.088	0.079	0.077	0.076
105	0.227	0.149	0.107	0.101	0.092	0.089	0.092
165	—	—	—	0.121	0.112	0.108	0.110
225	0.271	0.185	0.137	0.140	0.132	0.123	0.126
315	—	—	—	0.157	0.148	0.144	0.142
405	0.281	0.217	0.172	0.171	0.161	0.156	0.162
24 h	—	—	—	—	—	—	0.169

*Initial pH for all runs, 5.6; total dissolution time for each run is 405 min except for Run 11.

Run No.	1	2	3	4	7	11
Final pH	6.9	6.9	7.1	7.2	7.2	7.3

Total initial water volume, 1,500 mL; system open to atmosphere; sample size for each measurement, 10 mL; particle size, 0.60–0.83 mm; solid weight loaded, 70 g; V_S = 22.6 cm^3; revolution speed, 210 rpm.

Continuous dissolution was studied using 2.5-cm-inside-diameter plexiglass columns packed with fluorspar particles. Fine sand was placed in the bottom of the column to a depth of about 3 cm to eliminate end effects. Nylon netting was placed below the sand layer to prevent possible blocking of the outlet by fine particles. A solid-state Varistaltic pump was used to pump distilled water to a flask located above the column. The flask had an overflow drain to maintain a constant fluid head. All connections were made with Tygon flexible plastic tubing. Flow rates were adjusted by a hose clamp attached to the outlet tubing and measured by timing the volume of effluent.

To determine equilibrium solubilities, saturated solutions of fluorspar in a packed column were obtained by recirculating effluent through the column at 500 cm^3/min. This recirculation reduced the mass transfer resistance sufficiently for the liquid stream to reach equilibrium with the solid within a relatively short period of time. Saturated solutions were also obtained by allowing long contact time (e.g., 75 to 270 days) in stationary columns (cf. Table 2).

All the experiments were conducted at 20 ± 1°C. The fluoride concentration in the solution was measured using an Orion Model 94-09 fluoride specific electrode. Calcium ion concentration was determined by EDTA titration with Eriochrome blue black *R* as indicator. Calcium ion concentration was measured only for equilibrium solutions, since the column effluent was too dilute to be titrated accurately. All pH measurements were performed using a Sargent-Welch 3000 pH meter, which was frequently calibrated with standard reference buffer solutions of pH 4, 7 and 10.

Results

In order to evaluate the main mass transfer coefficient, k_{11}, the surface concentration C_{1S} and the bulk concentration C_1 must be known. When measuring these quantities, however, it was found in both batchwise and continuous packed bed experiments that there was a transient period during which C_{1S} decreased with dissolution time until a steady-state value was reached. As shown in Table 1, where the data from seven identical runs (of the total of 11) for a single sample of fluorspar are listed, repetition of batch experiments led to lower dissolution rates and ultimate fluoride concentrations. The reductions apparently diminished with subsequent runs. For example, there

Table 2. Saturation Fluoride Concentrations in Packed Columns of Fluorspar Particles

Particle Size mm	Contact Time day	$[F^-]$ Inside Column mM	$[Ca^{2+}]$ Inside Column mM	pH Inside Column
0.3–0.42	75	0.179	0.83	7.9
0.6–0.83	100	0.183	0.74	8.0
	270	0.178	—	—
		0.186*	—	7.8*
1.2–1.7	75	0.178	—	—
Average		0.180		

*Obtained by recirculation of effluent at 500 mL/min. Other data were measured in zero-flow rate columns (column initially filled with distilled water). All the experiments were conducted after aging process was completed, i.e., after about 80 hours dissolution in the packed column (cf. Figure A1).

was virtually no difference between Runs 7 and 11. The transient period was as long as about 60 hours for the packed bed operated at 50 cm³/min. This phenomenon is referred to as aging and is discussed in the Appendix.

The previous derivation of the equations to predict packed bed effluent compositions (Eqs. 23 and 24) relied on the assumption that C_{1S} was constant. Therefore, the value of C_{1S} after the transient period (i.e., after Run 6 in the batch experiments or 60 hours dissolution in the packed bed) is of interest to this study. This steady-state C_{1S} was measured and is shown in Table 2, where the measured value of equilibrium pH was predicted using K_{a1} and K_{a2}, as well as the carbonate concentration, which was calculated from K_{sp2} and the calcium ion concentration obtained from Eq. 9 or 10 (Qi, 1988). The average of five measurements gave: $C_{1S} = 0.181 \pm 0.005$ mM. Note that this is about one third the value (~0.5 mM) obtained for pure CaF_2 (Qi, 1988). Listed in Table 3 are the steady-state effluent fluoride concentrations at different flow rates and packing heights.

The saturation HCO_3^- concentration is calculated approximately from pH measurements to be $C_{2S} = 1.$ mM. Evidently, $C_{10} = 0$ for the influent stream of distilled water. Furthermore, the distilled water had pH = 5.6 and therefore should give approximately, $C_{20} = 2.5 \times 10^{-3}$ mM (Stumm and Morgan, 1981).

Validation of Theoretical Model

If the coupling effect is insignificant, i.e., the cross-term mass transfer can be neglected, then the dissolution system can be modeled by considering only one mass transfer coefficient. Analysis of batch dissolution data using a single mass transfer coefficient was attempted here by employing Eq. 23 and setting $k_{12} = 0$. Since the liquid volume was not constant due to sampling during the experiments, Eq. 23 is applied to the interval between two sampling times t_i and t_{i+1}:

$$\frac{C_{1S} - C_{1,i+1}}{C_{1S} - C_{1,i}} = \exp\left(- k_{11} a \frac{V_S}{V_{L,i}} (t_{i+1} - t_i) \right) \qquad (29)$$

where the subscript i represents the ith sampling; $V_{L,i}$ is the liquid volume between sampling times i and $i + 1$; and $C_{1,i}$ and $C_{1,i+1}$ are the fluoride concentrations of ith and $i+1$th samples, respectively.

Multiplying the above equation from $i = 0$ to $i = n$ gives:

$$\frac{C_{1S} - C_{1,n+1}}{C_{1S} - C_{10}} = \exp\left(- k_{11} a V_S \sum_{i=0}^{n} \frac{t_{i+1} - t_i}{V_{L,i}} \right) \qquad (30)$$

Therefore, if the preceding assumption of $k_{12} = 0$ is valid, we should obtain a straight line with a zero intercept when plotting

$$\log \frac{C_{1S} - C_{1,n+1}}{C_{1S} - C_{10}} \quad \text{vs.} \quad V_S \sum_{i=0}^{n} \frac{t_{i+1} - t_i}{V_{L,i}}$$

The data of Runs 6, 7 and 11, which are considered to have constant C_{1S}, should be used for the plot. Unfortunately, such a plot, as shown in Figure 2, demonstrates very weak linearity for the majority of the experimental data.

The fact that this simple treatment using a single mass transfer coefficient cannot accurately reflect the nature of the problem provides inducement for considering cross-term effects. A nonlinear regression, based on Eq. 23 and data of runs 6, 7 and 11, was performed to give $B_1 a = -4.60$ min^{-1}, $B_2 a = -0.27$ min^{-1}, and $B_3 = -0.81$ (Qi, 1988). The fit is compared with the experimental data in Figure 3. Since Eq. 23 involves three constants B_1, B_2, and B_3, which have to be determined experimentally, it might be viewed merely as a data fitting equation. To the contrary, the method developed below reduces the number of empirical constants to one main mass transfer coefficient, which incorporates the cross-term coupling effects by employing diffusion coefficient ratios.

Conventional mass transfer correlations for flow through a packed bed are generally represented by a dimensionless equa-

Table 3. Steady-State Results of Packed Column Dissolution at Different Packing Heights and Flow Rates*

Column Height (cm)	Voidage	Flow Rate cm³/min	Effluent [F⁻], mM	pH
12.5	0.50	50	0.053	7.0
		100	0.032	6.5
		200	0.020	6.1
		400	0.012	5.9
25.0	0.49	50	0.069	7.2
		100	0.050	6.8
	0.46	50	0.076	7.0
		100	0.052	6.5
		200	0.034	6.5
		300	0.028	6.3
		400	0.023	6.0
37.5	0.46	50	0.095	7.2
		100	0.079	6.8
		200	0.051	6.4
		300	0.038	6.4
50.0	0.45	0	0.183	7.8
		50	0.111	8.3
		100	0.089	7.8
		200	0.063	6.7

*ϕd_p = 0.59 mm; particle size, 0.60–0.83 mm; distilled water feed; pH of influent distilled water, 5.6.

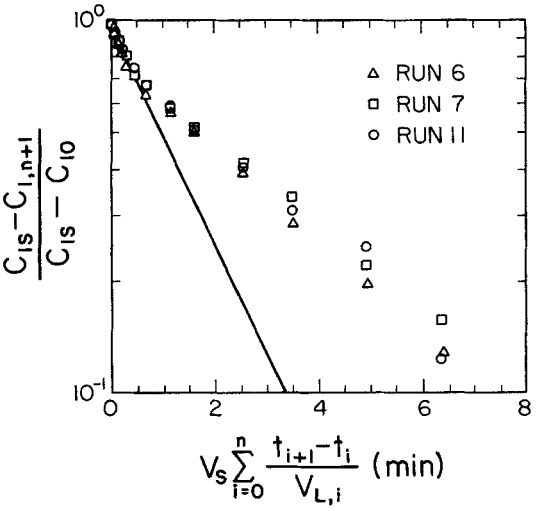

Figure 2. Conventional method of modeling, considering only the main-term mass transfer coefficient.

tion of the following form (van Krevelen and Krekels, 1948):

$$St \propto Re^{-n}Sc^{-m} \tag{31}$$

where m and n are constants; St is the Stanton number, defined as k/v, in which k is the sole relevant mass transfer coefficient (since such correlations were typically obtained for dissolution of single solute) and v is superficial velocity. Re is the modified Reynolds number, defined as $\phi d_p v/\nu$, in which ϕ is shape factor, d_p is particle diameter, and ν is kinematic viscosity. Sc is the Schmidt number, defined as ν/D, in which D is the diffusion coefficient.

By analogy to such correlations, the existence of the following relationship for the absolute values of main and cross mass transfer coefficients is expected:

$$St_{ij} \propto \pm Re^{-n}\,|Sc_{ij}|^{-m} \tag{32}$$

where St_{ij} and Sc_{ij} are the Stanton number and the Schmidt number obtained by replacing k and D with k_{ij} and D_{ij} in their definitions, respectively. Note that the Stanton and Schmidt numbers should have the same sign as D_{ij}.

Equation 32 can be reduced to:

$$k_{ij} \propto \pm |D_{ij}|^m \tag{33}$$

There is no apparent reason for m to depend on the species, although much of the simplicity of our proposed method would be lost if m were different for each species. Using the above relation, Eqs. 25 to 28 become:

$$B_1 = -\left(\frac{1}{2} + \frac{1}{2}\left(\frac{D_{22}}{D_{11}}\right)^m\right) \cdot \left(1 + \sqrt{1 - \frac{4\left[\left(\frac{D_{22}}{D_{11}}\right)^m - \left(\frac{D_{12}D_{21}}{D_{11}^2}\right)^m\right]}{\left[1 + \left(\frac{D_{22}}{D_{11}}\right)^m\right]^2}}\right) k_{11} \tag{34}$$

$$B_2 = -\left(\frac{1}{2} + \frac{1}{2}\left(\frac{D_{22}}{D_{11}}\right)^m\right) \cdot \left(1 - \sqrt{1 - \frac{4\left[\left(\frac{D_{22}}{D_{11}}\right)^m - \left(\frac{D_{12}D_{21}}{D_{11}^2}\right)^m\right]}{\left[1 + \left(\frac{D_{22}}{D_{11}}\right)^m\right]^2}}\right) k_{11} \tag{35}$$

$$B_3 = \frac{1 \pm \frac{1}{C_r}\left(\frac{|D_{12}|}{D_{11}}\right)^m - \frac{1}{2}\left[1 + \left(\frac{D_{22}}{D_{11}}\right)^m\right]\left(1 + \sqrt{1 - \frac{4[(D_{22}/D_{11})^m - (D_{12}D_{21}/D_{11}^2)^m]}{[1 + (D_{22}/D_{11})^m]^2}}\right)}{[1 + (D_{22}/D_{11})^m]\sqrt{1 - \frac{4[(D_{22}/D_{11})^m - (D_{12}D_{21}/D_{11}^2)^m]}{[1 + (D_{22}/D_{11})^m]^2}}} \tag{36}$$

$$B_4 = \frac{-1 \pm C_r\left(\frac{|D_{21}|}{D_{11}}\right)^m + \frac{1}{2}\left[1 + \left(\frac{D_{22}}{D_{11}}\right)^m\right]\left(1 - \sqrt{1 - \frac{4[(D_{22}/D_{11})^m - (D_{12}D_{21}/D_{11}^2)^m]}{[1 + (D_{22}/D_{11})^m]^2}}\right)}{[1 + (D_{22}/D_{11})^m]\sqrt{1 - \frac{4[(D_{22}/D_{11})^m - (D_{12}D_{21}/D_{11}^2)^m]}{[1 + (D_{22}/D_{11})^m]^2}}} \tag{37}$$

The signs for the terms $(|D_{12}|/D_{11})^m$ and $(|D_{21}|/D_{11})^m$ in Eqs. 36 and 37, respectively, also depend upon the cross diffusion coefficients.

The electrolyte diffusion coefficients D_{ij} can be computed by (Lasaga, 1979, 1981; Cussler, 1976):

$$D_{ij} = \delta_{ij}D_i^0 - \frac{z_i z_j C_i D_i^0}{\sum_{k=1}^{3} z_k^2 C_k D_k^0}(D_j^0 - D_3^0), \quad (i, j = 1, 2) \tag{38}$$

where

$$\delta_{ij} = \begin{cases} 0 \text{ when } i \neq j \\ 1 \text{ when } i = j \end{cases}$$

$$D_i^0 = \frac{RT}{|z_i|F^2}\lambda_i^0, \quad (i = 1, 2, 3) \tag{39}$$

Using the data available for ionic conductivities at 25°C (Perry and Chilton, 1973):

for F^- ion: $\lambda_1^0 = 55.4$ cm^2/ohm/equivalent
for HCO_3^- ion: $\lambda_2^0 = 44.5$ cm^2/ohm/equivalent
for Ca^{2+} ion: $\lambda_3^0 = 59.5$ cm^2/ohm/equivalent

we obtain:

$$D_{11} = D_1^0\left(1 - \frac{0.2232}{1 + 0.9051C_2/C_1}\right) \tag{40}$$

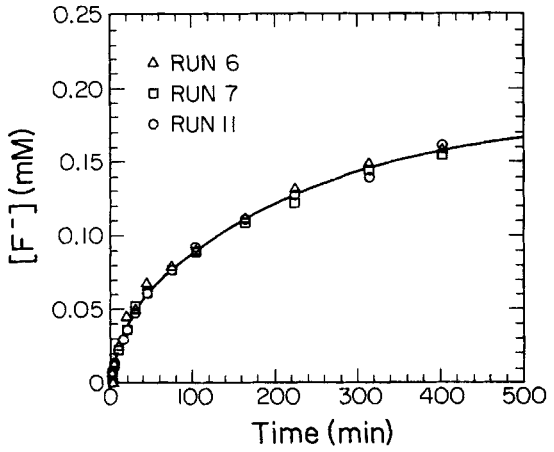

Figure 3. Batch dissolution model vs. experimental data.

$$D_{12} = -\frac{0.1284 D_1^0}{1 + 0.9051 C_2/C_1} \tag{41}$$

$$D_{21} = -\frac{0.2466 D_2^0}{1 + 1.105 C_1/C_2} \tag{42}$$

$$D_{22} = D_2^0\left(1 - \frac{0.1418}{1 + 1.105 C_1/C_2}\right) \tag{43}$$

Negative values of cross diffusion coefficients D_{12} and D_{21} in Eqs. 41 and 42 lead to negative values of k_{12} and k_{21}. Accordingly, the terms $(|D_{12}|/D_{11})^m$ and $(|D_{21}|/D_{11})^m$ in Eqs. 36 and 37, respectively, should have negative signs. From Eqs. 34 to 37 and 40 to 43, B_1/k_{11}, B_2/k_{11}, B_3, and B_4 can be calculated and, therefore, k_{11} can be evaluated from concentration data.

Equations 40–43 suggest that the diffusion coefficients and, therefore, the mass transfer coefficients are functions of the concentration ratio of ions 1 and 2, i.e., F^- and HCO_3^-. It should also be noted from Eqs. 34–37 and 39–43 that B_1/k_{11}, B_2/k_{11}, B_3 and B_4 are functions of the concentration ratio and the conductivity ratios. The conductivity ratios should be constant by the Walden's rule (Harned and Owen, 1958; Robinson and Stokes, 1959). In order to apply Eqs. 23 and 24, the values of B_1, B_2, B_3, and B_4 averaged over the range of the concentration ratio should be used.

The surface area per unit volume of solid can be evaluated by (Perry and Chilton, 1973):

$$a = \frac{6}{\phi d_p} \tag{44}$$

where ϕ is shape factor; d_p is average particle diameter; and ϕd_p can be obtained from the Kozeny-Carman equation (Carman, 1951; Cadle, 1965; Stockham and Fochtman, 1977; Subramanian and Arunachalam, 1980):

$$\frac{h}{L} = \frac{150}{(\phi d_p)^2}\frac{(1-\epsilon)^2}{\epsilon^3}\frac{\nu v}{g} \tag{45}$$

where h is the measured head loss over the packing height L.

The approach suggested here combines the effects of fairly involved equilibria and multicomponent mass transfer. It has a single adjustable constant (k_{11}) to be evaluated from experimental data. Through that one parameter, effects of variations in flow rate, temperature, solvent background composition, pH, and other conditions may be assessed. The following paragraphs describe the procedure for correlating continuous flow and dissolution in a packed bed.

For Eqs. 40 to 43, $C_1/C_2 = C_{1S}/C_{2S} = 0.18$ can be assumed for a given τ. As a first approximation, we also assume that the film mass transfer concept may be applied, i.e., $k_{ij} = D_{ij}/\ell$, where ℓ is the apparent film thickness. The film theory implies that in Eqs. 31 and 32, $m = 1$.

Substituting these values in Eqs. 40 to 43 to obtain D_{11}, D_{12}, D_{21}, and D_{22}, then using $m = 1$ in Eqs. 34 to 36 result in $B_1/k_{11} = -1.0$, $B_2/k_{11} = -0.7$, $B_3 = -0.59$.

These constants and the data given in Table 3 are employed to calculate k_{11} from Eq. 23. To evaluate k_{11} as a function of temperature, it is necessary to estimate the dependence of saturation fluoride concentration on temperature via Eq. 10 using standard entropy and enthalpy changes (Qi, 1988). Neglecting the slight difference of the temperature dependence of the aging effect, Eqs. 21 to 24 predict that C_1/C_2 is not significantly affected by temperature. Hence, the data from Peng (1988) obtained at the Reynolds number of about 1.0 and temperatures of 2 to 49°C, are used to evaluate k_{11} and to examine its dependence on Sc_{11}.

The above-stated calculations allow log (St_{11}) to be plotted against log (Re) at constant Sc_{11} to obtain value of n. Since this procedure requires m to be known, however, one begins with the previously-stated values of B_1/k_{11}, B_2/k_{11}, B_3, and m as a first approximation. Such evaluated n then can be used to plot log $(St_{11}Re^n)$ versus log (Sc_{11}) for a new value of m, which is then used to recalculate B_1/k_{11}, B_2/k_{11}, and B_3. This procedure is repeated until values of m and n are consistent. In this manner, we obtain ultimately

$$n = 0.69, \quad m = 1.2$$

and

$$B_1/k_{11} = -1.00, \quad B_2/k_{11} = -0.69, \quad B_3 = -0.25$$

Comparisons of the calculated values using these correlations with experimental data are shown in Figures 4 and 5. For further details of the correlation, see Qi (1988).

Discussion and Conclusions

Dissolution of fluorspar can be viewed as a process consisting of two steps. The first is the chemical reaction or hydration step and the second is the diffusion step in which hydrated species transfer into bulk fluid. The chemical reaction occurring in a very thin film of the solvent adjacent to the solid surface is believed to be sufficiently rapid for this film to be saturated with the species released from the dissolution. Therefore, the rate-determining step is the mass transfer from the saturated film to bulk solution.

As Eqs. 1 to 7 show, more than eight species are potentially relevant in $CaF_2 - CaCO_3$ dissolution. These eight species present in the saturated film transfer to bulk solution in rates that satisfy the electroneutrality of the solution. The equilibrium calcium concentration listed in Table 2 shows that in this film, the

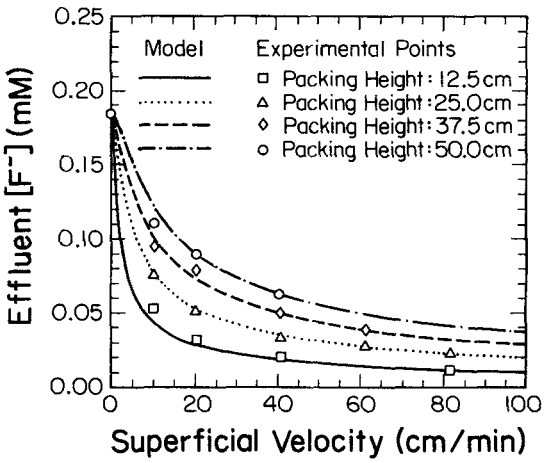

Figure 4. Steady-state model vs. experimental data for packed columns.

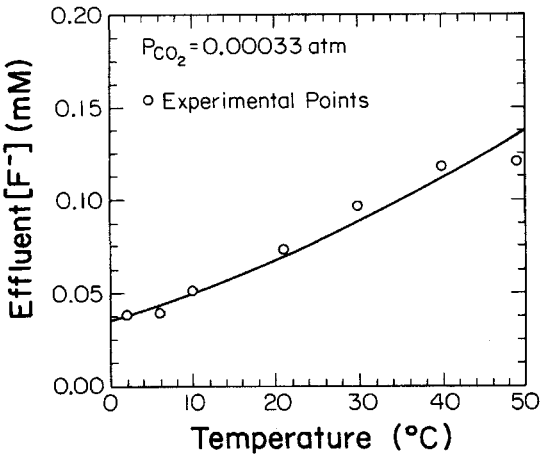

Figure 5. Steady-state model vs. experimental data (Peng, 1988) for packed columns at several temperatures.

The solid line represents the computed values from the model.

dissolution of $CaCO_3$ plays an important role since the calcium concentration far exceeds the value contributed by CaF_2 dissociation alone. The pH increase (i.e., from 5.6 of distilled water to 8 as shown in Table 2) also demonstrated the importance of the following two reactions of calcite (Berner and Morse, 1974):

$$H^+ + CaCO_3 \rightarrow Ca^{2+} + HCO_3^- \qquad (46)$$

$$2H^+ + CaCO_3 \rightarrow Ca^{2+} + H_2CO_3 \qquad (47)$$

since the consumption of H^+ by formation of HF can be easily shown to be negligible.

Fortunately, the surface reaction film can be treated as a system only involving F^-, HCO_3^-, and Ca^{2+}, since other species can be shown by theory and/or experiments to be negligible compared to these three species (Qi, 1988). Despite the fact that the main and cross diffusion coefficients for many ternary system can be calculated and measured accurately, the application of those coefficients requires one to know the concentration gradients in order to calculate the mass transfer fluxes. These gradients are difficult to determine for many dissolution systems. The approach presented in this paper provides a method for resolving the complicated situations.

The value obtained for n (0.69) in this study is very close to that obtained by Williamson et al. (1963) and Wilson and Geankoplis (1966) in their studies of packed-bed dissolution of benzoic acid spheres. They found that in the range of 0.0016 to 55 for the packed bed Reynolds number, and Stanton number (or k/v) was proportional to $Re^{-2/3}$, a relationship theoretically derived by Pfeffer (1964). The dependence of mass transfer coefficient on the Reynolds number also partially validates a tacit, but crucial, assumption that the dissolution of fluorspar is mass-transport-controlled. Furthermore, the dependence of dissolution rate on revolution speed (as mentioned in the Experimental section) was still observed even though the Reynolds numbers in the batch experiments were 3 to 4 orders of magnitude greater than those in the column. This leads us to conclude that the possibility of a surface reaction kinetic constraint is low even in the batch experiments, where the mass transfer rate is greatly enhanced by agitation.

The values of m appearing in the literature are usually less than one, while $m = 1.2$ was found here. Neglecting the temperature effect on aging may have introduced some inaccuracy in the correlation. Furthermore, since the data were obtained over a limited range (about ½ decade of Sc) and the variation of Sc_{11} was induced solely by temperature, $m = 1.2$ should not be expected to be universally applicable.

Notation

a = surface area per unit volume of solid
$a_{CO_2(aq)}$ = activity of aqueous carbon dioxide
B_1, B_2, B_3, B_4 = constants in steady-state rate equations
C_i = molar concentrations of species i
C_{iS} = surface concentration of species i
C_{i0} = influent or initial concentration of species i
$C_f = (C_{1S} - C_{10})/(C_{2S} - C_{20})$
$\bar{C}_i = (C_i - C_{i0})/(C_{iS} - C_{i0})$
C = instantaneous effluent fluoride concentration
C_0 = initial fluoride concentration
$C_{S,\text{eff}}$ = effective surface concentration of F^-
C_S = initial surface concentration of F^-
D = diffusion coefficient
D_i^0 = tracer diffusion coefficient of species i
D_{ij} = elements of multicomponent diffusion coefficient matrix
d_p = average particle size
F = Faraday constant, 96,400 C/equiv., $C^2 = J \cdot s/ohm$
f = fraction of surface fluoride unable to dissolve
h = head loss
J_i = molar flux of species i
K_b, K_c = dissociation constants of CaF^+ and $CaHCO_3^+$
K_{a1}, K_{a2} = first and second carbonic dissociation constants
K_{sp1}, K_{sp2} = solubility product of calcium fluoride, calcite
K_w = dissociation constant of water
k = mass transfer coefficient
k_{ij} = elements of multicomponent mass transfer coefficient matrix
k_1, k_{-1} = attachment rate constants of surface complex
L = length of packed column
ℓ = film or diffusion layer thickness
m, n = empirical constants of correlation
Q = volumetric flow rate
R = gas constant
S, S_0 = surface covered by adsorption, and total surface
T = absolute temperature
t = dissolution time
V = volume of packed column
V_L = volume of liquid in batch
V_S = volume of solid in batch
v = superficial velocity

Greek letters

γ_i = activity coefficient of species i
ϵ = voidage
θ = sum of rate constants, $k_1 + k_{-1}$
λ_i^o = equivalent conductivity of ion i in infinite dilution
ν = kinematic viscosity
τ = variable in rate equations
ϕ = shape factor

Subscripts

0 = influent or initial
1, 2, 3 = F^-, HCO_3^-, Ca^{2+}
L = liquid
S = saturation or solid

Literature Cited

Anderson, D. E., and D. L. Graf, "Multicomponent Electrolyte Diffusion," *Ann. Review Earth Planetary Sci.*, **4,** 95 (1976).

Bates, R. L., *Geology of the Industrial Rocks and Minerals,* Dover Publications, New York (1969).

Berner, R. A., and J. W. Morse, "Dissolution Kinetics of Calcium Carbonate in Sea Water: IV. Theory of Calcite Dissolution," *Amer. J. Sci.*, **274,** 108 (1974).

Brown, D. W., and C. E. Roberson, "Solubility of Natural Fluorite at 25°C," *U.S. Geol. Survey J. Res.*, **5,** 509 (1977).

Bruun C., D. Moe, and H. E. L. Madsen, "Study on the Dissolution Behavior of Calcium Fluoride," *Scand. J. Dent. Res.*, **91,** 247 (1983).

Bryant, S. L., R. S. Schechter, and L. W. Lake, "Mineral Sequences in Precipitation/Dissolution Waves," *AIChE J.*, **33,** 1271 (1987).

Butler, J. N., *Ion Equilibrium—A Mathematical Approach,* Addison-Wesley, London (1964).

Cadle, R. D., *Particle Size—Theory and Industrial Applications,* Reinhold Publishing, New York (1965).

Carman, P. C., *Symp. on New Methods for Particle Size Determination in Subsieve Range.*, ASTM, Philadelphia (1951).

Chander, S., C. C. Chiao, and D. W. Fuerstenau, "Transformation of Calcium Fluoride for Caries Prevention," *J. Dent. Res.*, **61,** 403 (1982).

Christoffersen, M. R., J. Christoffersen, and J. Arends, "Kinetics of Dissolution of Calcium Hydroxyapatite, VII. The Effect of Fluoride Ions," *J. Crystal Growth,* **67,** 107 (1984).

Crundwell, F. K., "Effect of Iron Impurity in Zinc Sulfide Concentrates on the Rate of Dissolution," *AIChE J.*, **34,** 1128 (1988).

Cussler, E. L., *Multicomponent Diffusion,* Elsevier, Amsterdam (1976).

Deitz, V. R., H. M. Rootare, and F. G. Carpenter, "The Surface Composition of Hydroxylapatite Derived from Solution Behavior of Aqueous Suspensions," *J. Colloid Sci.*, **19,** 87 (1964).

Diniz, R. G., R. G. de Araujo, and A. J. de Albuquerque, "Development of a Simplified Water Fluoridation Technique for Small Communities," *Bull. Pan Am. Health Organ.*, **16,** 224 (1982).

Fleisch, H., and W. F. Neuman, "Mechanisms of Calcification: Role of Collagen, Polyphosphates, and Phosphatase," *Amer. J. Physiol.*, **200,** 1296 (1961).

Franke, M. D., W. R. Ernst, and A. S. Myerson, "Kinetics of Dissolution of Alumina in Acidic Solution," *AIChE J.*, **33,** 267 (1987).

Harned, H. S., and B. B. Owen, *The Physical Chemistry of Electrolytic Solutions,* 3rd ed., Reinhold, New York (1958).

Jacobson, R. L., and D. Langmuir, "Dissociation Constants of Calcite and $CaHCO_3^+$—from 0 to 50°C," *Geochim. et Cosmochim. Acta,* **38,** 301 (1974).

Kanaya, Y., P. Spooner, J. L. Fox, W. I. Higuchi, and N. A. Muhammad, "Mechanistic Studies on the Bio-availability of Calcium Fluoride for Remineralization of Dental Enamel," *Int. J. Pharm.*, **16,** 171 (1983).

Kim, J. L., and E. L. Cussler, "Dissolution and Reprecipitation in Model Systems of Porous Hydroxyapatite," *AIChE J.*, **33,** 705 (1987).

Krebs, R., M. Sardin, and D. Schweich, "Mineral Dissolution, Precipitation, and Ion Exchange in Surfactant Flooding," *AIChE J.*, **33,** 1371 (1987).

Lagerlof, F., E. P. Saxegaard, P. Barkvoll, and G. Rolla, "Effects of Inorganic Orthophosphate and Pyrophosphate on Dissolution of Calcium Fluoride in Water," *J. Dent. Res.*, **67,** 447 (1988).

Larson, T. E., and A. M. Buswell, "Calcium Carbonate Saturation Index and Alkalinity Interpretations," *J. Amer. Water Works Assoc.*, **34,** 1664 (1942).

Lasaga, A. C., "The Treatment of Multi-component Diffusion and Ion Pairs in Diagenetic Fluxes," *Amer. J. Sci.*, **279,** 324 (1979).

———, "The Treatment of Multi-component Diffusion and Ion Pairs in Diagenetic Fluxes: Further Comments and Clarification," *Amer. J. Sci.*, **281,** 981 (1981).

Maier, F. J., and E. Bellack, "Fluorspar for Fluoridation," *J. Amer. Water Works Assoc.*, **49,** 34 (1957).

Maier, F. J., "Advances in the Use of Fluorspar for Fluoridation," *J. Amer. Water Works Assoc.*, **52,** 97 (1960).

Peng, C., "Bench-Scale Column Studies of Fluoridation Using Mixed-Grade Fluorspar," MS Thesis, Ohio State Univ., Columbus (1988).

Perry, R. H., and C. H. Chilton, *Chemical Engineer's Handbook,* 5th ed., McGraw-Hill, New York (1973).

Pfeffer, R., "Heat and Mass Transport in Multiparticle Systems," *Ind. Eng. Chem. Fund.*, **3,** 380 (1964).

Pinto, N. G., and E. E. Graham, "Multicomponent Diffusion in Concentrated Electrolyte Solutions: Effect of Solvation," *AIChE J.*, **33,** 436 (1987).

Qi, J., "Multicomponent Equilibrium and Mass Transfer: Applied to Dissolution of Fluorspar," PhD Thesis, Ohio State Univ., Columbus (1988).

Robinson, R. A., and R. H. Stokes, *Electrolyte Solutions,* 2nd ed., Butterworths, London (1959).

Rolla, G., and B. Ogaard, "Studies on the Solubility of Calcium Fluoride in Human Saliva," *Factors Relating to Demineralisation and Remineralisation of the Teeth,* S. A. Leach, ed., IRL Press Limited, Oxford (1986).

Rootare, H. M., V. R. Deitz, and F. G. Carpenter, "Solubility Product Phenomena in Hydroxyapatite-Water Systems," *J. Colloid Sci.*, **17,** 179 (1962).

Saska, M., and A. S. Myerson, "Crystal Aging and Crystal Habit of Terephthalic Acid," *AIChE J.*, **33,** 848 (1987).

Smith, A. N., A. M. Posner, and J. P. Quirk, "Incongruent Dissolution and Surface Complexes of Hydroxyapatite," *J. Colloid and Interface Sci.*, **48,** 442 (1974).

———, "A Model Describing the Kinetics of Dissolution of Hydroxyapatite," *J. Colloid and Interface Sci.*, **62,** 475 (1977).

Smith, L. W., and R. Taylor, "Film Models for Multicomponent Mass Transfer: A Statistical Comparison," *Ind. Eng. Chem. Fund.*, **22,** 97 (1983).

Snaeyink, V. L., and D. Jenkins, *Water Chemistry,* Wiley, New York (1980).

Stewart, W. E., "Multicomponent Mass Transfer in Turbulent Flow," *AIChE J.*, **19,** 398 (1973).

Stewart, W. E., and R. Prober, "Matrix Calculation of Multicomponent Mass Transfer in Isothermal Systems," *Ind. Eng. Chem. Fund.*, **3,** 224 (1964).

Stockham, J. D., and E. G. Fochtman, *Particle Size Analysis,* Ann Arbor Science Publishers, Ann Arbor (1977).

Stumm, W., and J. J. Morgan, *Aquatic Chemistry,* 2nd ed., Wiley, New York (1981).

Subramanian, P., and Vr. Arunachalam, "A Simple Device for the Determination of Sphericity Factor," *Ind. Eng. Chem. Fund.*, **19,** 436 (1980).

Suzuki, M. and K. Kawazoe, "Particle-to-Liquid Mass Transfer in a Stirred Tank with a Basket Impeller," *J. Chem. Eng. Japan,* **8,** 79 (1975).

Taylor, R., "Solution of the Linearized Equations of Multicomponent Mass Transfer," *Ind. Eng. Chem. Fund.*, **21,** 407 (1982).

Toor, H. L., "Solution of the Linearized Equations of Multicomponent Mass Transfer: I.," *AIChE J.*, **10,** 448 (1964).

———, "Solution of the Linearized Equations of Multicomponent Mass Transfer: II. Matrix Methods," *AIChE J.*, **10,** 460 (1964).

van Krevelen, D. W., and J. T. C. Krekels, "Rate of Dissolution of Solid Substances," *Rec. Trav. Chim.*, **67,** 512 (1948).

Weast, R. C., et al., eds., *Handbook of Chemistry and Physics,* 67th ed., CRC Press, Boca Raton, FL (1986).

Weller, J. M., R. M. Grogan, and F. E. Tippie, "Geology of the Fluorspar Deposits of Illinois," *Ill. State Geol. Surv. Bull.*, No. 76 (1952).

Wendt, R. P., "The Estimation of Diffusion Coefficients for Ternary Systems of Strong and Weak Electrolytes," *J. Phys. Chem.*, **69,** 1227 (1965).

Williamson, J. E., K. E. Bazaire, and C. J. Geankoplis, "Liquid-Phase Mass Transfer at Low Reynolds Numbers," *Ind. Eng. Chem. Fund.*, **2,** 126 (1963).

Wilson, E. J., and C. J. Geankoplis, "Liquid Mass Transfer at Very Low Reynolds Numbers in Packed Beds," *Ind. Eng. Chem. Fund.*, **5,** 9 (1966).

Woolf, L. A., "Multicomponent Diffusion in A System Consisting of A Strong Electrolyte Solute at Low Concentrations in An Ionizing Solvent," *J. Phys. Chem.*, **56,** 1166 (1972).

———, "Relationships between Diffusion Coefficients in A Three-Component System in Which Two Components Are Isotopically Related," *J. Phys. Chem.*, **56,** 2489 (1972).

Appendix: Decrease in Dissolution Rate Caused by Surface Concentration Reduction

Mineral dissolution commonly involves such factors as impurities, reprecipitation, surface complex formation, adsorption of ions on the surface, and polymorphic phase transformation. (See, for example, Kim and Cussler, 1987; Saska and Myerson, 1987; Franke et al., 1987; Krebs et al., 1987; Bryant et al., 1987; Crundwell, 1988.) Thus, the mechanism is more complex than for a pure solid, and almost every mineral has unique dissolution characteristics. This Appendix offers explanations on aging phenomena observed during fluorspar and other mineral dissolutions, from a viewpoint different than previous theories.

In 1987, Franke et al. reported that the dissolution rate of alumina in water and acidic solutions decreased as alumina experienced successive dissolution. A single sample in repeated identical batch dissolution experiments led to lower dissolution rates and lower apparent solubilities. Similar phenomena were also found in their packed column dissolution experiments. They postulated the possible formation of two surface species, AlOOH and $[Al(OH)_2]_2SO_4$, and suggested that these relatively insoluble species remained on the alumina to inhibit the dissolution. The empirical rate expression from their study, however, did not exhibit a saturation limit nor a solubility decrease due to aging.

Christoffersen et al. (1984) showed that the solubility and the dissolution rate of calcium hydroxyapatite ($Ca_{10}(PO_4)_6(OH)_2$) were reduced, apparently by the adsorption of fluoride ions on the crystal surface. They modeled the adsorption of fluoride following the Langmuir approach. While their model represented the inhibitory effect of fluoride ions on the rate of dissolution for short times, it did not, however, account for the apparent reduction of the equilibrium solubility.

Smith et al. (1974, 1977) observed similar reductions of the solubility of hydroxyapatite in water and ascribed the reductions to a surface complex formed by hydrolysis of phosphate ions in the terminal planes of the crystal, a mechanism postulated earlier by Rootare et al. (1962) and Deitz et al. (1964). They believed that the release of ions by this hydrolysis reaction and a simultaneous formation of the surface complex, $Ca_2(HPO_4)(OH)_2$, accounted for the apparent solubility decrease. However, neither of them could give a quantitative model to explain the solubility decrease.

Chander et al. (1982), Kanaya et al. (1983), Rolla and Ogaard (1986), and Lagerlof et al. (1988) found that very low concentrations of inorganic phosphate and pyrophosphate considerably reduced the solubility and the dissolution rate of calcium fluoride. Chander et al. (1982) claimed that the adsorption of HPO_4^{2-} onto the crystal surface of calcium fluoride caused the reduction. This mechanism was also discussed by Fleisch and Neuman (1961).

In the study of fluoride dissolution, we observed the similar reduction in solubility and dissolution rate. As shown in Table 1 in the main text, the fluoride concentration at about 405 minutes decreased with each run from about 0.28 mM to about 0.16 mM, which is far below the value obtained for pure CaF_2 (0.5 mM) or fluorspar powder (0.31 mM) (Qi, 1988). In packed bed, the effluent fluoride concentration decreased with operation time to a steady state, as shown in Figure A1, where Column No. 2 was packed and operated in the same manner as No. 1 to replicate the phenomenon.

Two types of changes may occur on the dissolving surface of a fluorspar particle: decrease in the active sites for hydration as a result of dissolution, and change of surface chemical composition, e.g., due to formation of a complex. The decrease in the active sites is unlikely to cause a decrease in the ultimate fluoride concentration since the equilibrium should not be affected by the number of sites, but only by the partial molar Gibbs free energy. Therefore, the change of surface concentration seems to be more reasonable, since the reduction of both saturation concentration and dissolution rate was observed.

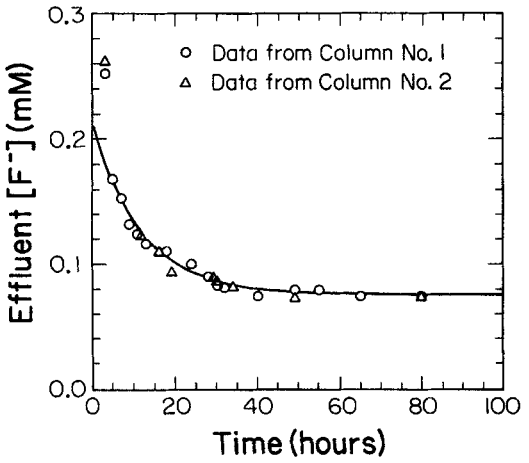

Figure A1. Decrease in effluent fluoride concentration with time to a steady-state value, showing the aging phenomenon.

Flow rate = 50 cm³/min; packing height = 25 cm; voidage = 0.46. Other experimental conditions are as stated in Table 3. The curve represents Eq. A9.

We speculate that the reduction of the surface fluoride concentration is caused by formation of a complex on the solid surface (e.g., $Ca(HCO_3)^+$) due to the presence of calcite. This complex, perhaps present only as a partial monolayer on the dissolving solid surface, binds to exposed fluoride sites. As a result, fewer fluoride ions are capable of dissolving. The presumed equilibrium of the rates of attachment and detachment of the complex to and from the solid surface, therefore, may significantly affect the surface fluoride concentration.

The rate of detachment of the complex from solid surface is taken to be proportional to the covered area, S, and likewise the rate of attachment is proportional to the uncovered surface area, $S_0 - S$, where S_0 is the total area. Therefore we have:

$$-\frac{dS}{dt} = k_1 S - k_{-1}(S_0 - S) \tag{A1}$$

where k_1 and k_{-1} are empirical rate constants. Note that the concentration of the detached complex in the bulk solution is included in k_{-1}. Let

$$f = S/S_0 \tag{A2}$$

We obtain:

$$-\frac{df}{dt} = k_1 f - k_{-1}(1 - f) \tag{A3}$$

with initial condition:

$$f = 0, \qquad \text{at } t = 0 \tag{A4}$$

Integrating Eq. A3 with Eq. A4 gives:

$$f = \frac{k_{-1}}{k_1 + k_{-1}} (1 - \exp[-(k_1 + k_{-1})t]) \tag{A5}$$

Assigning $C_{S,\text{eff}}(t)$ to the instantaneous surface fluoride concentration available for mass transfer, which is diminished by the presumed adhesion of the complex, we have

$$C_{S,\text{eff}}(t) = C_S(1 - f) \tag{A6}$$

where C_S is the surface fluoride concentration at $t = 0$, i.e., the surface fluroide concentration prior to formation of the complex. This concentration should be equal to that for aqueous fluoride in equilibrium with pure CaF_2, stated earlier at 0.5 mM.

Combining Eqs. A5 and A6 gives:

$$C_{S,\text{eff}}(t) = C_{S,\text{eff}}(\infty) + [C_S - C_{S,\text{eff}}(\infty)] \exp(-\theta t) \tag{A7}$$

where $C_{S,\text{eff}}(\infty) = C_S k_1/(k_1 + k_{-1}) = 0.18$ mM (cf. Table 2 in the main text) and $\theta = k_1 + k_{-1}$. Since the hydrodynamic conditions were kept constant during the column aging process, the mass transfer coefficients and therby B_i can be assumed constant. This may be seen in the main text by examining Eqs. 25–28. According to Eq. 23, the fluoride concentration ratio, $\bar{C}_i$, is therefore independent of aging time. When the influent stream contains no fluoride ($C_{i0} = 0$), we have:

$$\frac{C(t)}{C_{S,\text{eff}}(t)} = \text{constant} = \frac{C(\infty)}{C_{S,\text{eff}}(\infty)} \tag{A8}$$

where $C(t)$ is instantaneous effluent fluoride concentration. Combining Eqs. A7 and A8 yields:

$$C(t) = C(\infty) + [C(0) - C(\infty)] \exp(-\theta t) \tag{A9}$$

where $C(\infty) = 0.074$ mM (cf. Figure A1).

The constants in Eq. A9 can be found by regression analysis of the data in Figure 1A to be:

$$C(0) = 0.212 \text{ mM} \tag{A10}$$

$$\theta = 0.083 \text{ h}^{-1} \tag{A11}$$

Using these values, Eq. A9 is plotted in Figure 1A to show the representation of the experimental data.

If the surface fluoride reduction is caused by species inside the stagnant boundary layer adjacent to the solid surface, it follows that k_1 and k_{-1} should not depend much upon the hydrodynamic conditions of dissolution. They should be only related to the chemical nature of the adhesion. Therefore, Eq. A7 should be applicable to the batch dissolution aging process as well.

For the batch dissolution, Eq. 23 can be used with $\tau = a(V_S/V_L)t$ to show that the ratio

$$\frac{C(t) - C_0}{C_{S,\text{eff}} - C_0}$$

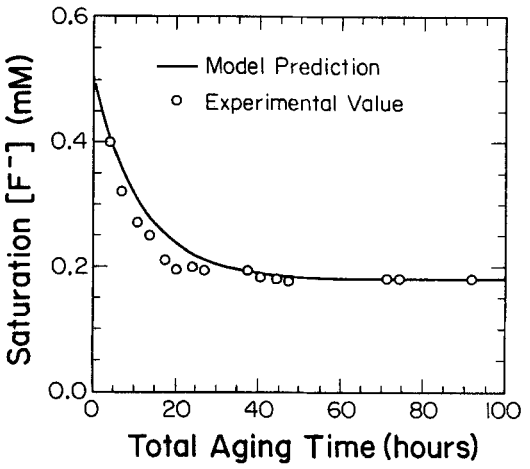

Figure A2. Direct application of the expression for instantaneous effective surface fluoride concentration.
Developed for packed column to the estimated data from batch experiments.

should be approximately equal for all runs shown in Table 1 with the same dissolution time, t, since the coefficients in Eq. 23, B_i, depend mainly on hydrodynamic conditions, and the solid/liquid volume ratio did not vary from run to run. (Since Eq. 23 is derived based on the constancy of $C_{S,\text{eff}}$, here it can only be used as an approximation by assuming that $C_{S,\text{eff}}$ does not change significantly during each run.) Note that here the initial fluoride concentration, C_0, is zero. Thus, the instantaneous surface concentration, $C_{S,\text{eff}}$, in batch experiments can be estimated from the bulk concentration and the final saturation concentration.

Consider the data obtained after the transient period of aging: Runs 7 and 11 in Table 1. The average fluroide concentrations of these two runs at 225 and 405 minutes are 0.124 and 0.159 mM, which are about 68% and 88% saturation, respectively, considering 0.18 mM to be the saturation concentration. According to the above analysis, it is reasonable to assume that the fluoride concentration at 225 and 405 minutes in each of the 11 runs reached 68% and 88% saturation, respectively. In this manner, the instantaneous surface fluoride concentrations are estimated from the data at 225 and 405 minutes and plotted in Figure A2, where the total aging time is simply the cumulative dissolution history. Equation A7, which applies to packed bed operation, is also plotted in that figure for comparison. As can be seen, the curve representing Eq. A7 shows very close agreement with the batchwise data points.

Note that this approach is conceptually different from previous reports, because the inhibitory effect is accounted for by progressive reduction of the effective surface concentration, rather than by a surface kinetic (blocking) effect. As a result, it is possible to account for observed reductions in both the initial rate of dissolution and the equilibrium solubility, rather than just the former. In addition, this approach yields one quantitative expression for the aging phenomenon observed in both batchwise and continuous packed-bed operations, although final proof of the proposed mechanism required detailed analysis of the structure and composition of the fluorspar surface.

Manuscript received Dec. 13, 1988, and revision received May 1, 1989.